Polymer 49 (2008) 4882–4888

Contents lists available at ScienceDirect

Polymer

journal homepage: www.elsevier.com/locate/polymer

Orientation-induced crystallization of poly(ethylene terephthalate) fibers with controlled microstructure

Jong Kahk Keum [a,1], Hye-Jin Jeon [a], Hyun Hoon Song [a,*], Jong-In Choi [b], Yang-Kug Son [c]

[a] Department of Advanced Materials, Hannam University, Daejeon, Republic of Korea
[b] R & D Business Labs, Technology Commercialization R & D Center, Hyosung Corporation Anyang, Republic of Korea
[c] R & D Business Labs, Production R & D Center, Hyosung Corporation Anyang, Republic of Korea

ARTICLE INFO

Article history:
Received 29 May 2008
Received in revised form 7 August 2008
Accepted 26 August 2008
Available online 11 September 2008

Keywords:
Orientation-induced crystallization
In-situ wide-angle X-ray diffraction
Controlled microstructure

ABSTRACT

Orientation-induced crystallization of PET fibers was studied by the *in-situ* wide-angle X-ray diffraction (WAXD) utilizing synchrotron radiation source combined with thermomechanical analysis. The non-crystalline as-spun fiber spun was heat-treated at 150, 165, 180 and 195 °C for 0.1 s under constrained condition. The heat-treatment allowed the fibers to have various amount of isotropic amorphous (IA), oriented noncrystalline (ON), and crystalline (Cr) phase. The structure evolution accompanying the crystallization of the fibers was then examined upon elevating temperature while the fiber length was held constant. The X-ray results clearly showed that the crystallization takes place first by ON phase (extended-chain crystallization) and then followed by the crystallization of IA phase (folded-chain crystallization). The on-set of extended-chain crystallization was dependent on the amount and degree of orientation of ON phase in the fiber that was derived from the various heat-treatment temperatures. It is also noted that the IA phase transforms into not only the CR phase but also the ON phase. The crystallization on the surface of preformed extended-chain crystals appeared to induce the spontaneous orientation of the chains. The thermomechanical data indicated that a stress emerges rapidly on fiber above glass transition temperature (T_g), which is associated with the entropic relaxation of the ON phase. The stress emerged on fiber then dropped drastically as the temperatures of fibers reached the temperatures of extended-chain crystallization, indicating that the stress drop is closely related with the extended-chain crystallization. The fibers heat-treated at the highest temperature showed the highest initial crystallinity but showed the slowest crystallization rate, resulting in the lowest final crystallinity among the fibers.

1. Introduction

Orientation-induced crystallization of polymer has been one of the important topics because of its practical implications in optimizing the polymeric properties and the processing conditions. Indeed, the usages of fibers [1–5] and films [6,7] are often based on the mechanical orientation of the chains and/or the subsequent crystallization by heat-treatment. Depending on these two processing conditions, fibers and films exhibit various orientations, crystalline structures and finally the mechanical properties of final products.

Among many polymers, in particular, a great deal of studies on orientation-induced crystallization of PET [8–16] have been carried out mainly because of its easiness of controlling microstructure due to the slow chain dynamics and high glass transition temperature. One of the most interesting structural features that can be found in the oriented PET is the existence of mesophase in the highly oriented noncrystalline structure [17–24]. This structure consisting of nearly extended chains can be preserved stable at the temperatures lower than T_g by quenching. Since the structure is highly unstable above T_g, however, it readily transforms into crystalline phase under heating and then induces the crystallization of random-coiled chains on top of it later.

The fast promotion of crystallization of extended chains can be explained in both thermodynamic and kinetic criteria [1]. Thermodynamically, the entropy of extended-chain conformation lower than that of random-coiled chain conformation leads to the decreased free energy barrier for primary nucleation. Kinetically, since an extended chain is closer to its conformation in the crystal, it has less kinetic barrier to overcome than the random-coiled chain has. As a result, crystallization of extended chains (extended-chain crystal or shish) is promoted and later induces the crystallization of the rest of chains (folded-chain lamella or kebab). Wu et al. systemically studied the relationship between chain microstructure

* Corresponding author.
E-mail address: songhh@hnu.ac.kr (H.H. Song).
[1] Present address: Macromolecular Science and Engineering, Case Western Reserve University, OH, United States.

0032-3861/$ – see front matter © 2008 Elsevier Ltd. All rights reserved.
doi:10.1016/j.polymer.2008.08.050

and mechanical properties whereby they divided the phases of polymer chain into three – isotropic amorphous, oriented non-crystalline and crystalline phase and the fraction of these phases were quantitatively resolved from two-dimensional (2D) wide-angle X-ray diffraction (WAXD) patterns [25,26].

Although extensive research on orientation-induced crystallization has been conducted, the nature of the crystallization process of oriented chains, i.e. the specific role of individual chains of different degrees of orientation on nucleation and crystallization, is not fully understood [1–5,9–18]. In this study, systematically controlled PET fibers possessing low and different amounts of crystals (Cr), oriented and unoriented amorphous (ON and IA) components were prepared. The crystallization processes of the fibers were then carefully examined utilizing the synchrotron X-ray scattering combined with the thermomechanical analysis. In particular, by separating the X-ray scattered intensities into IA, ON and Cr phases, the structural transformations could be thoroughly scrutinized.

2. Experimental

2.1. Preparation of sample

High-speed melt-spun (spun at 3200 m/min) PET fiber was obtained from Hyosung Corporation. The high-speed fiber spinning process produced the oriented noncrystalline fiber with 3.29 deniers. In order to control the microstructures of the fibers, the spun fibers were heat-treated by passing through the heating zone maintained at given temperatures above the typical cold-crystallization temperature ($T_{cc} \approx 135\,^{\circ}C$) – 150, 165, 180 and 195 °C. In this way the as-spun fibers were heat-treated only for 0.1 s at the given temperatures. During the heat-treatments, the length of fibers was held constant and the resultant deniers of each fiber were 3.18, 3.19, 3.18 and 3.16, respectively. Through this controlled process of heat-treatment, the fibers possess different amounts of crystals and noncrystalline structures of oriented and nonoriented chains. The intrinsic viscosity of PET chip before spinning and heat-treatment was 0.64 dl/g.

2.2. Instrumentations and measurements

In-situ WAXD measurements upon heating were performed at the 4C1 X-ray beamline in Pohang Accelerator Laboratory (PAL) using a synchrotron X-ray source (2.5 GeV, 150 mA). The temperature of the fiber was elevated inside the heating block while holding the fiber length constant. The heating rate was 5 K/min. The wavelength of X-ray beam was 1.6083 Å and the collimated beam size was 0.3 mm × 0.3 mm. Two-dimensional (2D) WAXD patterns were collected using a position-sensitive area detector with resolution of 1204 × 1152 pixels. Each pixel corresponded to 100 μm. The exposure time of each 2D WAXD pattern was 23 s and the time for data storage was 7 s. By using two ion chambers along the X-ray beam path before and after sample, all 2D WAXD patterns were corrected for sample absorption, air and other background scattering. In order to investigate the cold-crystallization behavior of fiber, DSC (MDSC, TA *Inc.*) was used. The scan speed was 5 K/min and the measurements were carried out while maintaining the sample length constant. Thermomechanical analysis was also carried out to investigate the thermal behavior of ON phase using tensile testing machine (Shimatzu, AG-5000 G). The changes of stress imposed on fibers upon elevating temperature could be detected by using the tensile testing machine (Shimatzu, AG-5000 G) attached with a heating device. The mode for this measurement was stress relaxation mode and the applied pre-strain was ≈0.1%. The data collection time for the stress measurement was 1 s.

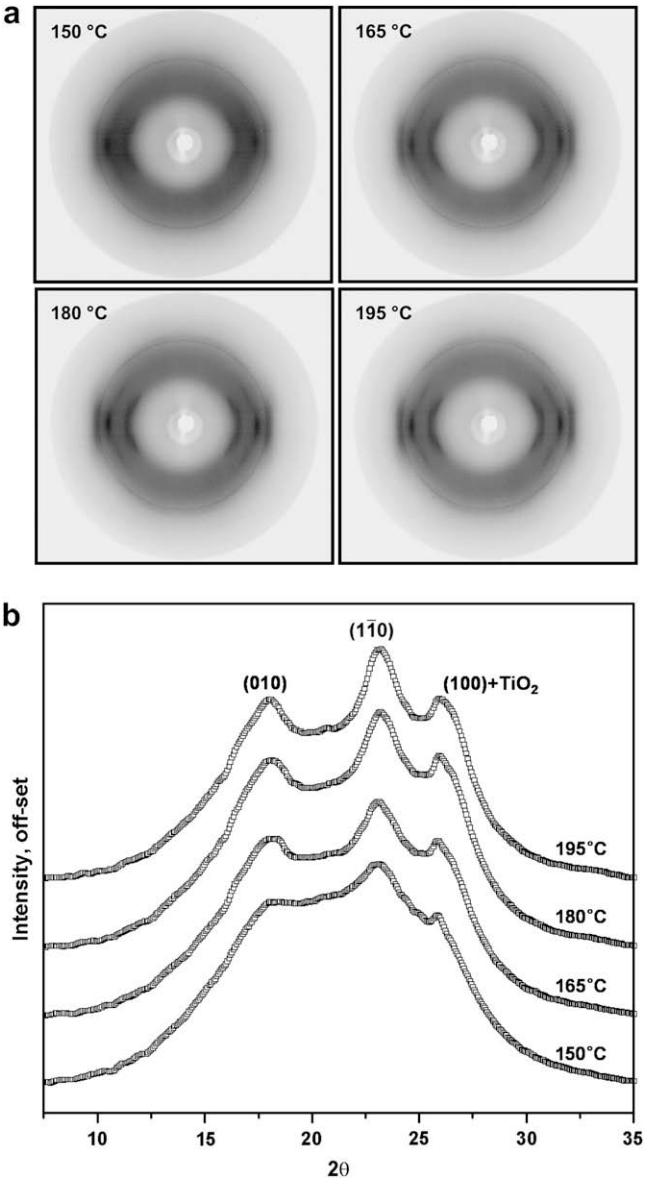

Fig. 1. (a) 2D WAXD patterns of heat-treated fibers collected at room temperature and (b) equatorial 1D WAXD patterns extracted from the 2D WAXD patterns in Fig. 1 (a).

3. Results and discussions

3.1. WAXD results

Fig. 1(a) shows 2D WAXD patterns of differently heat-treated fibers collected at room temperature. We note that the faint but sharp crystalline reflection rings found in the 2D WAXD patterns are due to the added TiO_2. Integrated equatorial one-dimensional (1D) WAXD profiles (−15° to +15°) taken from the 2D WAXD patterns in Fig. 1(a) are also shown in Fig. 1(b). We also note that the 1D and 2D WAXD patterns of as-spun fiber (spun at 3200 m/min) without heat-treatment only showed oriented but diffused diffraction feature at around the equator without any crystalline reflection. As the fibers were heat-treated, however, the WAXD patterns of each fiber clearly indicated the formation of crystals that are aligned along the fiber direction. It is thought that, even though the heat-treatment time of fiber was relatively short, the high heat-treatment temperatures above the cold-crystallization temperature of melt-quenched PET ($T_{cc} = 135\,^{\circ}C$) were enough to induce the crystallization. Also, crystalline reflections were found

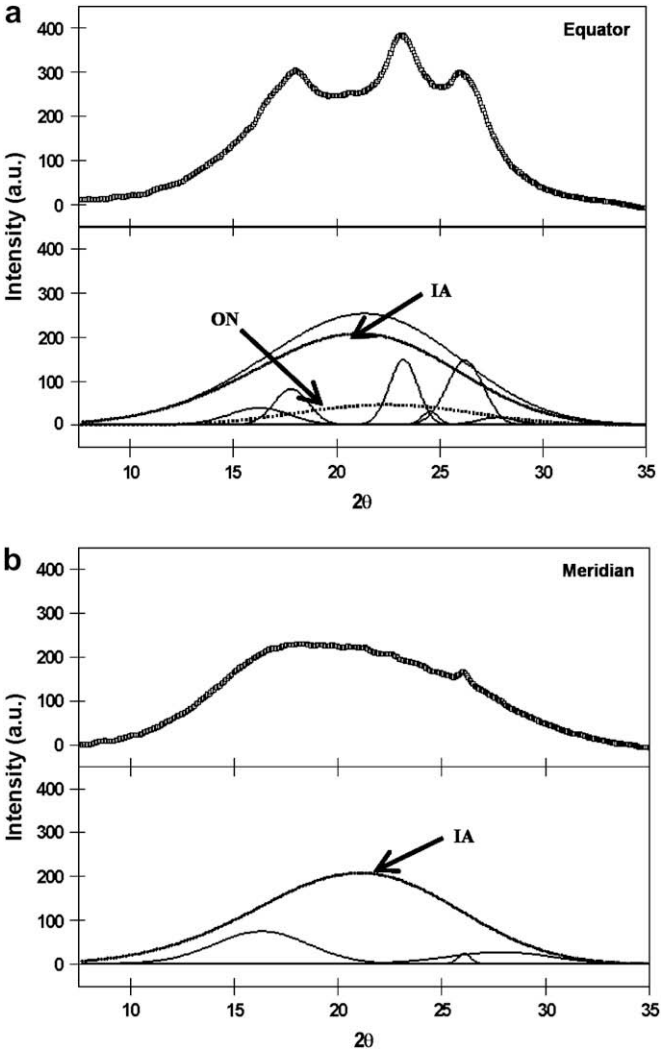

Fig. 2. Curve-fitting results of (a) equatorial and (b) meridianal WAXD pattern.

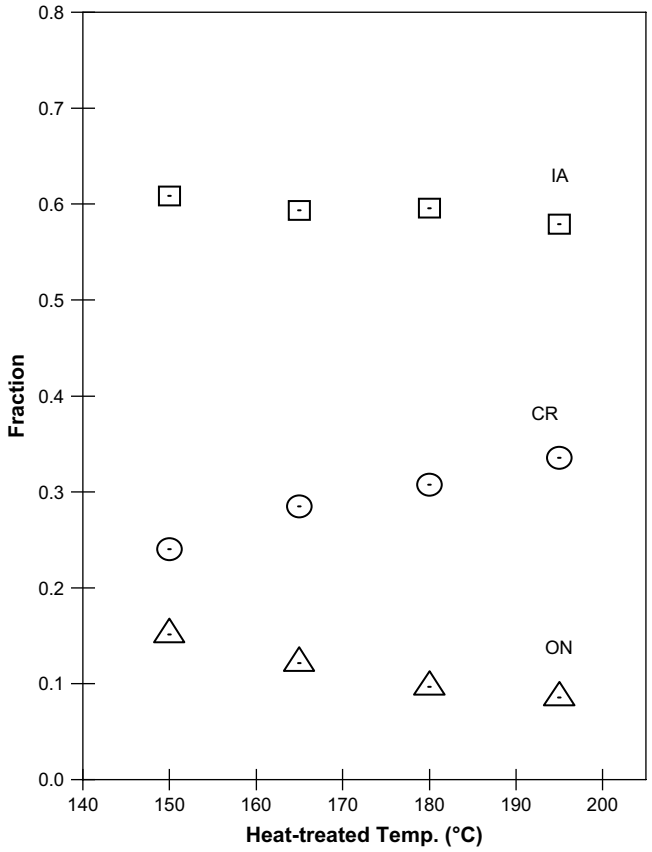

Fig. 3. Initial fractions of IA, ON and Cr phases of the heat-treated fibers obtained from Fig. 2(a) and (b).

to intensify as the heat-treatment temperature increased, implying that the higher thermal energy (higher heat-treatment temperature) could lead more fractions of chains to crystallize.

In order to examine the internal chain structures of the fibers and their subsequent changes upon crystallization in greater detail, the 2D WAXD patterns of each fiber were analyzed as follows [25,26]. First, it was assumed that the structure of the oriented fibers with heat-treament consisted of three phases; isotropic amorphous (IA), oriented noncrystalline (ON), and crystalline (CR) phase. The contributions of each phase to WAXD intensities were then resolved from the curve-fits of equatorial and meridianal reflections using Gaussian functions. Since the diffused reflections of IA and ON phases are overlapped in WAXD profile, it was assumed that the noncrystalline reflection in the total meridianal reflection is only responsible for IA phase and this contribution is everywhere the same along azimuthal angle in the 2D WAXD patterns. The curve-fits at the equator and meridian are exemplified in Fig. 2(a) and (b), respectively. By adopting the curve-fitted profile of IA phase in meridianal reflection into the curve-fit of the equatorial reflection, the overlapped IA and ON contributions could be separated. Finally, the fractions of each phase were calculated as

$$X_{IA} = \frac{A_{IA}}{(A_{IA} + A_{ON} + A_{Cr})} \quad (1)$$

$$X_{ON} = \frac{A_{ON}}{(A_{IA} + A_{ON} + A_{Cr})} \quad (2)$$

$$X_{Cr} = \frac{A_{Cr}}{(A_{IA} + A_{ON} + A_{Cr})} \quad (3)$$

$$X_{IA} + X_{ON} + X_{Cr} = 1 \quad (4)$$

where A_{IA}, A_{ON} and A_{Cr} being the reflection areas of each phase, respectively, and X_{IA}, X_{ON} and X_{Cr} being the fraction of IA, ON and Cr phases, respectively. Based on this procedure, the derived fractions of each phase are depicted in Fig. 3. In the figures, it is first noted that, at the ambient temperature before heating, the differences in ON and Cr fraction between the fibers of different heat-treatment temperature are clearly seen. IA fraction, on the other hand, remained nearly constant for all the fibers. This indicates that the ON phase in as-spun fiber was mainly responsible for the initial gain of the Cr phase by the heat-treatment while IA phase remained at a dormant stage. Since ON phase possessed lowered conformational entropy and thereby the reduced free energy barrier for crystallization, their crystallization seems to be promoted by allowing ON to Cr phase transformation within the relatively short heat-treatment time scale (0.1 s). However, considering the applied heat-treatment temperatures that are higher than the cold-crystallization temperature of melt-quenched PET ($T_{cc} \approx 135\,^{\circ}C$), it is believed that the time for heat-treatment was too short for IA phase to overcome the nucleation barrier at the surface of preformed extended-chain crystals. It is also seen that more fraction of ON phase transformed into Cr phase when the heat-treatment

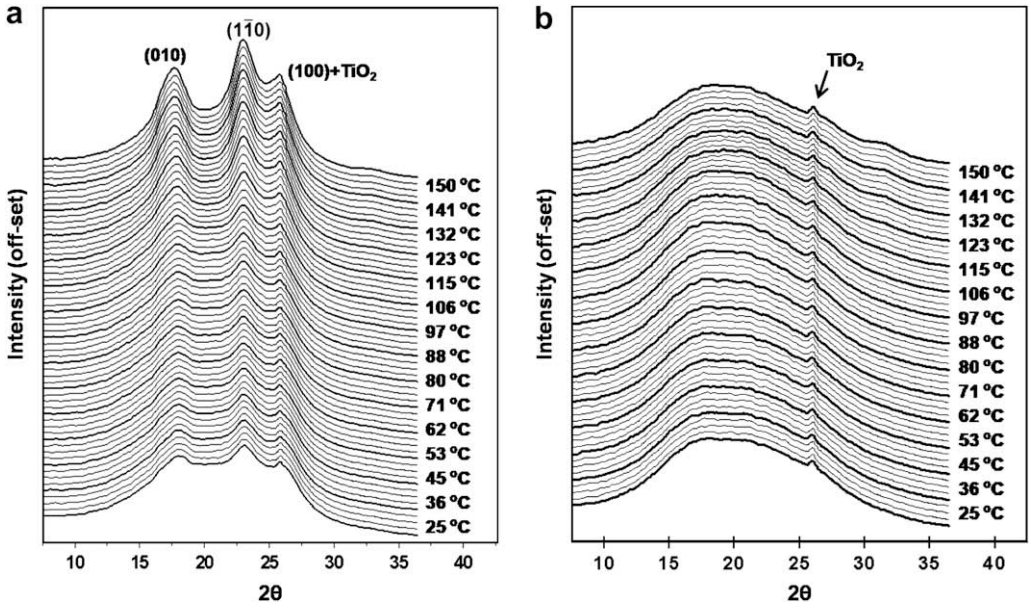

Fig. 4. Temperature evolution of *in-situ* 1D WAXD profiles of heat-treated fiber at 180 °C taken at (a) the equator and (b) meridian.

temperature was higher. This can be explained as follows. As the crystallization of polymer chain is a kinetic event following a pathway and the chains in fiber have their own kinetic barrier for crystallization (more extended chain will have less kinetic barrier for crystallization), only the chains with the degree of extension higher than a certain critical value will crystallize at the given crystallization condition. The higher heat-treatment temperature, therefore, decreases the critical degree of chain extension value since the chain mobility increases and thus the kinetic barrier decreases as temperature increases. Based on this argument, it is anticipated that more fraction of ON phase in as-spun fiber can transform into Cr phase during heat-treatment as the heat-treatment temperature increases.

The applied short-term heat-treatment and the fast quenching to the temperature below T_g can generate frozen structure, i.e. frozen phases, which are in their pathway to an equilibrium state. These structures of frozen phases can be controlled by the heat-treatment temperature as explained previously. The frozen phases can be activated again upon elevating temperature above T_g. Here, *in-situ* WAXD technique was very useful to investigate the structural evolutions in the fibers having the unfavorable frozen phases upon elevating temperature. Fig. 4(a) and (b) shows the changes of equatorial and meridianal reflections upon elevating temperature taken from the 2D WAXD patterns of the heat-treated fiber at 180 °C as an example. Typical three main reflections of PET such as (010), ($\bar{1}$10) and (100) are observed in the equatorial reflections. As the temperature was increased further above T_g, the reflections were intensified. In meridianal reflection, however, any notable crystalline reflection of PET did not appear. The weak but sharp crystalline reflection marked with arrow in the meridianal reflection is due to the added small amount of TiO_2 and the reflection of it was overlapped with (100) reflection in equatorial reflections. In order to separate the three phases (IA, ON and Cr phases) the equatorial reflections of each fiber were analyzed using the procedure mentioned previously and the results are shown in Fig. 5(a). Also, the on-set temperatures of the phase transformations (crystallization), IA to Cr phase and ON to Cr phase transformations, are shown in Fig. 5(b). The on-set temperatures in Fig. 5(b) were obtained from (a). It is seen that the fractions of each phase begin to change as the temperature increases above glass transition temperature, $T_g \approx 80$ °C. The changes in these three phases, decrease in IA and ON phases and increase of Cr phase, are associated with the phase transformation between the phases as a result of the applied heat energy. Most of all, it is seen that the decreases of ON fraction and the increases of Cr fraction in each fiber are coincided while the IA phase of each fiber begins to decrease at the higher temperatures than the ON and Cr phases do. These observations demonstrate that the initial crystallization in each fiber is mainly associated with the ON to Cr phase transformation (extended-chain crystallization) while IA phase still remained at a dormant stage.

Previously, it was discussed that the ON phase in as-spun fiber has different kinetic barriers to overcome depending on the degree of chain extension. As the degree of chain extension increases, its crystallization is prompted due to the decreased kinetic barrier. Since more extended chains in ON phase would have crystallized as the heat-treatment temperature increases, the remaining less extended chains should lead to the increase in crystallization temperature as shown in Fig. 5(a) and (b). Differently from the extended-chain crystallization, the IA phase remained unchanged. Previously, it was also suggested that short-term heat-treatment was not enough to induce the crystallization of IA phase. This was due to the higher nucleation barrier of IA phase. As seen in Fig. 5(a) and (b), IA phase finally begins to crystallize $T \approx 96$ °C for all fibers. This temperature is much lower than the typical cold-crystallization temperature of melt-quenched PET ($T_{cc} \approx 135$ °C). It is thought that the nucleation of IA phase is accelerated by the preformed extended-chain crystals. Thus, it can be envisaged that, upon elevating temperature, the ON phase forms extended-chain crystal first due to lowered kinetic barrier (or free energy barrier) while IA phase forms probably the folded-chain lamella later by way of secondary nucleation on top of extended-chain crystal.

We also observe that the ON phase begins to increase at temperatures immediately following the on-set of IA phase crystallization. It is quite unusual to observe that the chains are spontaneously oriented in the absence of any external force. The observation strongly suggests that the IA phase transforms not only into CR phase but also into the ON phase. It is believed that the transformation of IA phase into ON phase is probably associated with the anisotropic growth of lamellar crystals. As discussed previously, the nucleation of IA crystallization is on the surface of preformed extended-crystals that limits the lamellar crystals to

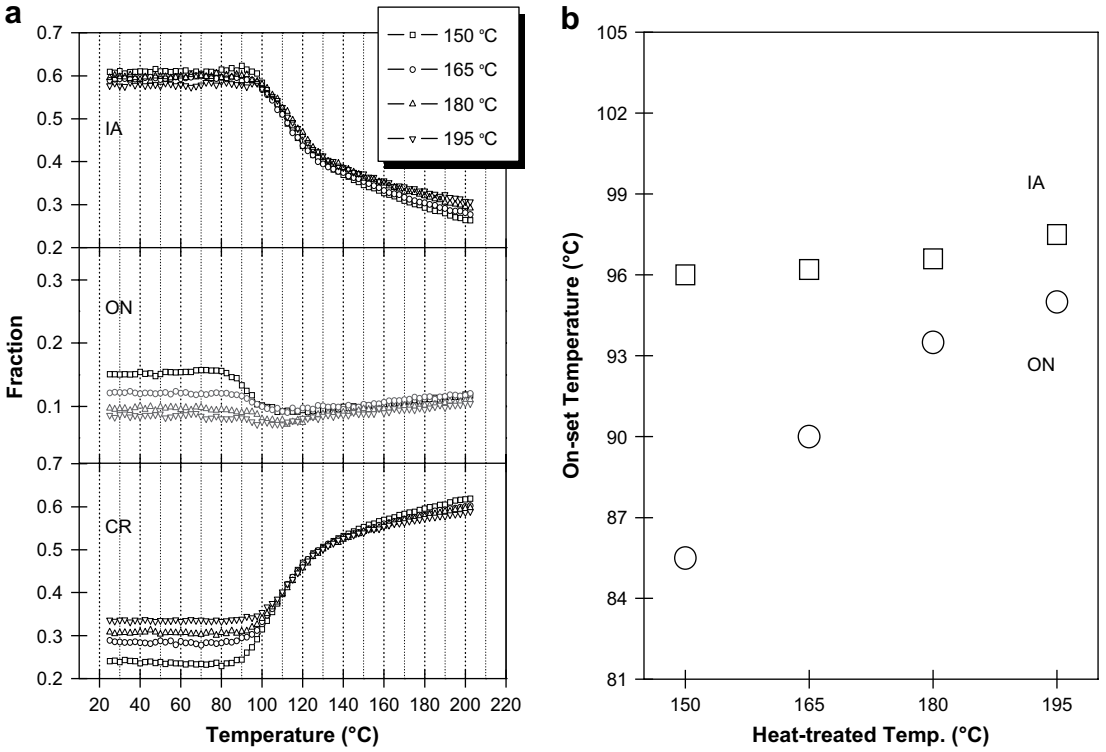

Fig. 5. (a) *In-situ* changes of fractions of IA, ON and Cr phase and (b) the on-set temperatures of IA to Cr and ON to Cr phase transformation.

grow in the transverse direction with the folded chains parallel to the fiber axis. Such an anisotropic growth of the crystals would induce the orientation of the remaining IA phase.

3.2. DSC results

The cold-crystallization of short-term heat-treated fibers has also been investigated utilizing differential scanning calorimetry (DSC) under constrained condition. In this case, transformations from IA or ON phase to Cr phase are appeared in the form of heat dissipation, e.g., cold-crystallization ($-\Delta H$, exothermic peak), upon heating. Also, if the total amount of phase transformation is associated with the total amount of heat dissipated (exothermic peak area), the kinetic barrier for the phase transformation (crystallization) is with the cold-crystallization temperature. In other words, the peak area increases as the total amount of phase transformation increases while the cold-crystallization temperature increases as the kinetic barrier of the phase transformation increases. DSC heating thermograms of each fiber showing cold-crystallization are depicted in Fig. 6. Also, the exothermic peak area ($-\Delta H$), on-set and maximum cold-crystallization temperature derived from the curve in Fig. 6 are listed in Table 1. It is seen that the exothermic peak area decreases as the heat-treatment temperature increases while the on-set and maximum cold-crystallization temperature increase. These are again due to the different heat-treatment of as-spun fibers as discussed previously. Since more ON fraction transformed into Cr phase during heat-treatment as heat-treatment temperature increased exothermic peak area should decrease. Also, as heat-treatment temperature increased more extended ON phase transformed into Cr phase during heat-treatment and thus cold-crystallization temperature should increase.

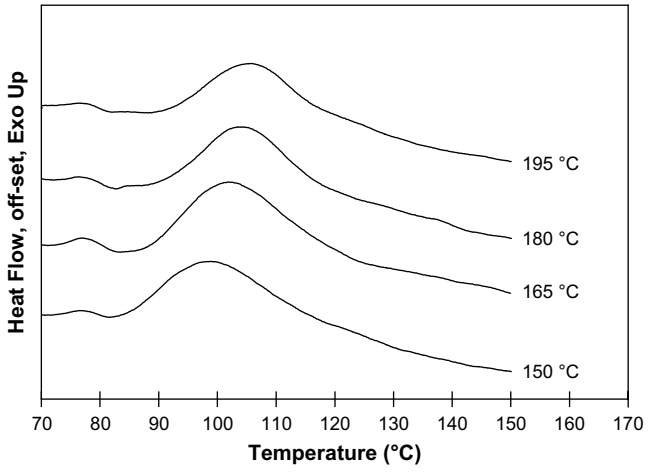

Fig. 6. DSC cold-crystallization behavior of each fiber.

3.3. Thermo mechanical analysis

When oriented noncrystalline fiber is heat-treated above its T_g, the contraction of fiber usually takes place accompanying the chain disorientation. This is due to the reduced entropy of extended chains in fiber and the reduced entropy can be compensated by relaxing back to random-coiled chain conformation. This entropic relaxation process accompanies the relaxation of stored stress in fiber. However, when the fiber length is held constant during the heat-treatment, the stored stress emerges in the fiber to compensate the contraction and the emerging stress can be recorded by

Table 1
Summary of DSC cold-crystallization results of each fiber

Heat-treated temperature (°C)	Cold-crystallization		
	$-\Delta H$ (J/g)	On-set (°C)	Maximum (°C)
150	20.0	82.7	100.2
165	19.3	86.7	103.5
180	17.5	88.4	105.3
195	15.7	90.5	106.9

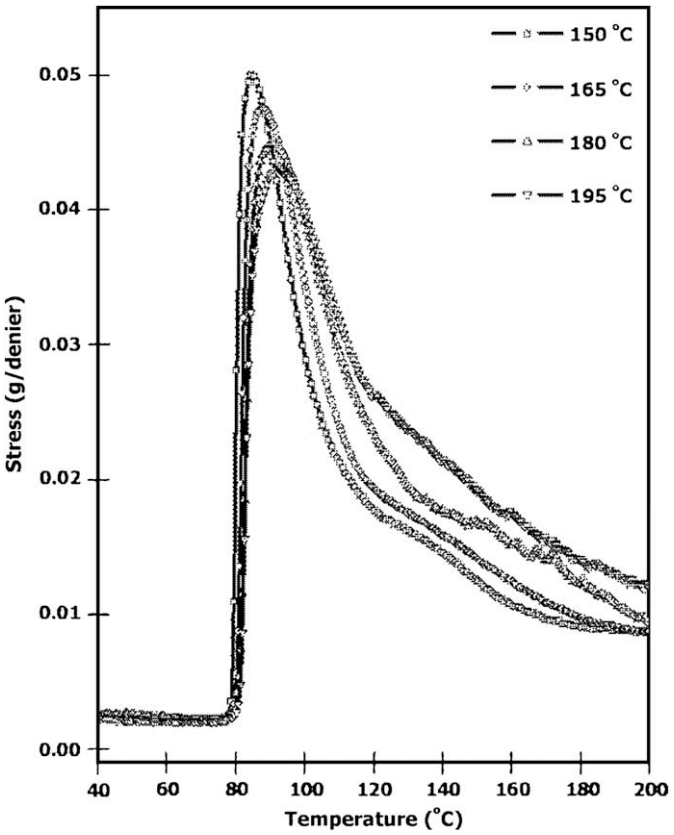

Fig. 7. (a) *In-situ* stress changes emerged in each fiber during elevating temperature.

thermomechanical analysis. In Fig. 7, results of thermomechanical analysis of each fiber are plotted. Also, the results are summarized in Table 2. As shown in the figure, the stress emerged on fiber begins to increase drastically at around glass transition temperature ($T_g \approx 80$ °C). This indicates that the extended chains become tensed due to the appearance of stored stress. It is also seen that the stress emerging on fiber becomes higher when the heat-treatment temperature decreases. This is apparently associated with the amount of ON phase remained in fiber as well as the degree of extension of ON phase. When the heat-treatment temperature is low, the fiber shall possess more fraction of ON phase and also higher degree of chain extension, resulting in higher stress in fiber. Recalling the results of WAXD (crystallinity gain and crystallization temperature) and DSC results (cold-crystallization peak area and temperature), it is apparent that the fraction of ON phase and the degree of extension are higher with the fibers of lower heat-treatment temperature.

One interesting feature that can be found in thermomechanical data is that the stresses in each fiber begin to drop rapidly as the temperature reaches about 83.9, 87.3, 90.9 and 93.4 °C, respectively. Since the fiber was constrained, and thus the chain relaxation is limited, it can be thought that the relaxation of stress is orginating from other effect. When compared with the WAXD results, it is seen that the on-set temperatures of stress drop are closely matching the respective extended-chain crystallization temperatures of each fiber (Table 2). This represents that the decrease of stress are evidently associated with extended-chain crystallization. The mechanism related to dimensional change upon heating has been controversially discussed in several papers [27–31]. In our previous report, the dimensional changes of oriented PET upon heating were noted and were attributed to the conformational change from gauche to trans state through the crystallization of oriented chains [19]. It is also noted that the decrement rate of the stress differs depending on the heat-treatment temperatures. The slopes are apparently representing the crystallization rate, where the fiber heat-treated at the highest temperature is showing the slowest crystallization rate. Furthermore, the final amount of CR phase (crystallinity) becomes the lowest in the fibers of highest heat-treatment temperature, even though the initial value of CR phase was the highest among the fibers (see Fig. 3). As discussed previously, the preformed crystals during the heat-treatment promote the nucleation of crystals but they appear to play a role in retardation of the crystal growth afterwards, eventually resulting in the lower crystallinity in fibers of higher heat-treatment temperature (see CR phase in Fig. 5(a)).

Table 2
On-set of crystallization temperature measured by thermomechanical analysis ($T_{c,TMA}$), WAXD ($T_{c,WAXD}$) and the stress maxima of thermomechanical analysis

Heat-treated temperature (°C)	$T_{c,TMA}$ (°C)	$T_{c,WAXD}$ (°C)	Max stress (mg/denier)
150	83.9	85.1	49.8
165	87.3	89.9	47.4
180	90.9	93.5	45.8
195	93.4	95.0	42.9

4. Conclusions

Orinetation-induced cold-crystallization process was thoroughly examined upon elevating temperature of the fibers that possess systematically controlled initial structures of three phases (CR, ON and IA). Time-resolved WAXD technique using synchrotron radiation source combined with thermomechanical analysis revealed that the crystallization takes place first by ON phase and followed by the IA crystallization. The on-set of ON crystallization depended on the heat-treatment temperature, i.e. the degree of orientation and amount of remaining ON phase. The IA phase crystallization, on the other hand, showed nearly the same on-set temperature regardless of the fiber heat-treatment temperature. It was also noted that the IA phase transforms not only into CR phase (crystallization) but also into ON phase. The presence of the extended-chain crystals formed during the short time heat-treatment and raising temperature accelerated the crystal nucleation of IA phase but at the same time reduced the crystal growth rate, resulting in the lowest final crystal content in the fibers of highest heat-treatment temperature. Thermomechanical analysis also proved to be a useful technique to monitor the microstructural changes in the fibers. Thermomechanical data showed that the stress originating from entropy relaxation emerges rapidly on fiber prior to the crystallization of ON phase. Most interestingly, the stress on fiber began to drop drastically as the temperatures of fibers reached crystallization temperature of ON phase. This indicated that the rapid stress drop is closely associated with extended-chain crystallization rather than the entropic chain disorientation.

Acknowledgements

This work was supported by Korea Research Foundation Grant (KRF-2004-041-D0020). The X-ray scattering was performed at the 4C1 and 4C2 beamlines of Pohang Accelerator Laboratory.

References

[1] Keller A, Kolnaar HWH, Meijer HEH. Processing of polymers, vol. 18. New York: VCH; 1997.
[2] Zachmann HG, Stuart HA. Makromol Chem 1960;41:131.
[3] Ziabicki A, Kawai H. High-speed fiber spinning. New York: Intersciences; 1985.
[4] Zaroulis JS, Boyce MC. Polymer 1997;38:1303.
[5] Llana PG, Boyce MC. Polymer 1999;40:6729.
[6] Beake BD, Leggett GJ. Polymer 2002;43:319.

[7] Chmelka BF, Schmidt-Rohr K, Spiess HW. Macromolecules 1993;26:2282.
[8] Bonart R. Kolloid-Z 1966;213:1.
[9] Bonart R. Kolloid-Z 1966;213:16.
[10] Bonart R. Kolloid-Z 1968;231:438.
[11] Asano T, Seto T. Polym J 1973;5:72.
[12] Asano T, Baltá-Calleja FJ, Flores A, Tanikaki M, Mina MF, Sawatari C, et al. Polymer 1999;40:6475.
[13] Blundell DJ, MacKerron DH, Fuller W, Mahendrasingam A, Martin C, Oldman RJ, et al. Polymer 1996;37:3303.
[14] Mahendrasingam A, Martin C, Fuller W, Blundell DJ, Oldman RJ, Harvie JL, et al. Polymer 1999;40:5553.
[15] Mahendrasingam A, Martin C, Fuller W, Blundell DJ, Oldman RJ, Mackerron DH, et al. Polymer 2000;41:1217.
[16] Yamaguchi T, Komoriyama K, Ohkoshi Y, Urakawa H, Gotoh Y, Terasawa T, et al. J Polym Sci Part B Polym Phys 2005;43:1090.
[17] Shaofeng R, Wang Z, Burger C, Chu B, Hsiao BS. Macromolecules 2002;35:10102.
[18] Keum JK, Kim J, Lee SM, Song HH, Son Y-K, Choi J-I, et al. Macromolecules 2003;36:9873.
[19] Keum JK, Song HH. Polymer 2005;46:939.
[20] Yeh GSY, Geil PH. J Macromol Sci 1967;B1:235.
[21] Yeh GSY, Geil PH. J Macromol Sci 1967;B1:251.
[22] Gorlier E, Haudin JM, Billon M. Polymer 2001;42:9541.
[23] Welsh L, Blundell DJ, Windle AH. Macromolecules 1998;31:7562.
[24] Kawakami D, Hsiao BS, Burger C, Ran S, Avila-Orta C, Sics I, et al. Macromolecules 2005;38:91.
[25] Wu G, Jiang J-D, Tucker PA, Cuculo JA. J Polym Sci Part B Polym Phys 1996;34:2035.
[26] Wu G, Yoshida T, Cuculo JA. Polymer 1998;39:6473.
[27] Pereira JRC, Porter RS. Polymer 1984;25:877.
[28] Alfrey T, Mark H. J Phys Chem 1942;46:112.
[29] Bosley DE. J Polym Sci Part C 1967;20:77.
[30] Mandelkern L, Roberts DE, Diorio AF, Posner AS. J Am Chem Soc 1959;81:4148.
[31] Grebowicz JS, Brown H, Chuah H, Olvera JM, Wasiak A, Sajkiewicz A, et al. Polymer 2001;42:7153.